

TR/77

SEPTEMBER 1977

THE NUMERICAL SOLUTION OF TWO-DIMENSIONAL
MOVING BOUNDARY PROBLEMS USING
CURVILINEAR CO-ORDINATE TRANSFORMATIONS.

by

R. M. FURZELAND

w9260406

ABSTRACT

A numerical method is described for the solution of two-dimensional moving boundary problems by transforming the curved, fixed and moving boundaries in the original co-ordinate system (x,y) into an orthogonal or, in general, nonorthogonal curvilinear system (ξ,η) such that the curved boundaries become (ξ,η) co-ordinate lines. All computations are then carried out in the transformed region using a fixed, rectangular (ξ,η) mesh which corresponds to a moving, non-rectangular (x,y) mesh. A one-phase, two-dimensional problem is solved by using two different such transformations and the results are compared with those from finite-element, enthalpy and isotherm migration methods.

Introduction

In two (and higher) space dimensions, moving boundary problems (MBPs) involve the solution of partial differential equations over regions with curved, moving and fixed boundaries. Standard finite-difference or finite-element approximations are inaccurate near such curved boundaries and, in order to maintain accuracy, special treatments are necessary. In recent years, a great deal of interest has been shown in the solution of partial differential equations subject to curved, fixed boundaries where the original co-ordinate system (x,y) is transformed into an orthogonal or, in general, nonorthogonal system (ξ,η) such that the curved boundaries become (ξ,η) co-ordinate lines. Associated with this transformation is the generation of a curvilinear (x,y) mesh spacing corresponding to a regular, straight-lined (ξ,η) spacing. Since the new co-ordinates are chosen so as to fit the original region's shape, they are often called 'body-fitted' or 'natural' co-ordinates.

The overheads involved in using such transformations are the need to solve the subsidiary mesh generation problem and the increased complexity of the transformed governing equation and boundary conditions. In return for these overheads such methods have several important advantages, since the numerical approximation is now over a simple, straight-lined bounded region with no loss of accuracy near the boundaries. Also, direct control over the (x,y) mesh spacing is now available thus enabling a finer mesh ('zoning') to be used in subregions of special interest (e.g. near moving boundaries (MBs) or singularities) and a coarser mesh to be used for the rest of the region. Further, the techniques can be preprogrammed for a general class of regions resulting in automatic mesh generation schemes.

For MBPs, where the region changes with time, a fixed (ξ, η) mesh which corresponds to a moving (x, y) mesh can be used for all time. The movement of the boundary and mesh points in the original region is reflected only through changes in x and y at the corresponding, fixed (ξ, η) points at each time step. This concept combines the moving mesh features of an Eulerian representation of the governing equations with that of a fixed mesh, Lagrangian one. The model problem treated is a one-phase, two-dimensional MBP in a rectangle, the fourth side of which is the MB. The problem is solved by transforming all the boundaries, including the MB, into fixed (ξ, η) co-ordinate lines. The techniques used suggest obvious extensions to regions with four curved sides.

2. Body-fitted, curvilinear co-ordinate transformations

Consider the transformation of a two-dimensional, four-sided region, with co-ordinates (x,y) , into a rectangular region, with co-ordinates (ξ,η) Fig. 1.

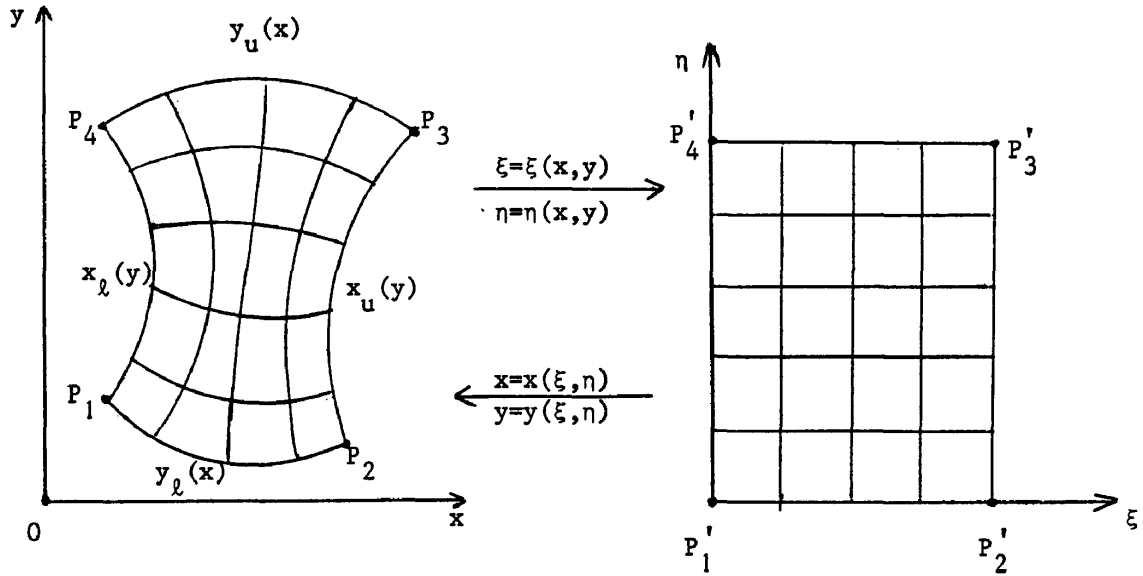


Figure 1. Transformation from original (x,y) to transformed (ξ,η) region.

The use of orthogonal transformations for the solution of flow problems in curved regions is well-known. For such problems one wishes to solve (say) Laplace's equation for the potential function $\phi(x,y)$

$$\nabla_{x,y}^2 \phi \equiv \phi_{xx} + \phi_{yy} = 0, \quad (2.1)$$

and an orthogonal, curvilinear system can be generated from the solution of the 'inverse' Laplace equations

$$\nabla_{\xi,\eta}^2 x = 0, \quad \nabla_{\xi,\eta}^2 y = 0. \quad (2.2)$$

Derivatives of ϕ with respect to x and y are given by

$$\phi_x = \phi_\xi / h_1, \quad \phi_y = \phi_\eta / h_2, \quad (2.3)$$

$$\text{where } h_1 = (x_\xi^2 + y_\xi^2)^{\frac{1}{2}}, \quad h_2 = (x_\eta^2 + y_\eta^2)^{\frac{1}{2}}. \quad (2.4)$$

Thus (2.1) is transformed into

$$\frac{1}{h_1 h_2} \left[\frac{h_2}{h_1} \phi_{\xi} \right]_{\xi} + \frac{1}{h_1 h_2} \left[\frac{h_1}{h_2} \phi_{\eta} \right]_{\eta} = 0. \quad (2.5)$$

Recent applications of this method have been given by Hung and Brown [13].

A particular case of (2.2) and (2.5) occurs if ξ, η are complex conjugates, a well-known example of this being $\xi \equiv \phi$ and $\eta \equiv \psi$, the potential and stream functions. Use of the Cauchy-Riemann

conditions reduces the solution of (2.2) and (2.5) to the solution of

$$\Delta_{\phi, \psi}^2 x = 0, \quad \nabla_{\phi, \psi}^2 y = 0, \quad (2.6)$$

over the rectangular (ϕ, ψ) region. This idea of exchanging the dependent and independent variables has long been in use, Thorn and Apelt [183], and has recently been extended by Boadway [3]. Interchange of dependent and independent variables forms the basis of the Isotherm Migration methods used for MBPs, see Crank and Gupta [7], Crank and Crowley [6]. Conformal transformations possess the useful property that the Laplacian operator remains invariant and methods based on these transformations have been applied to two-dimensional MBPs by Kroeger and Ostrach [14].

For nonorthogonal co-ordinate systems the transformed equations are more complicated. Derivatives of $\phi(x, y)$ are given by:

$$\phi_x = (y_{\eta} \phi_{\xi} - y_{\xi} \phi_{\eta}) / J, \quad (2.7)$$

$$\phi_y = (y_{\eta} \phi_{\xi} - x_{\xi} \phi_{\eta}) / J, \quad (2.8)$$

where J is the Jacobian $x_{\xi} y_{\eta} - x_{\eta} y_{\xi} \neq 0$, and where the

following differential relations have been used

$$\xi_x = y_{\eta} / J, \quad \xi_y = -x_{\eta} / J, \quad (2.9)$$

$$\eta_x = -y_{\xi} / J, \quad \eta_y = x_{\xi} / J. \quad (2.10)$$

Using the above relation, Laplace's equation for $\phi(x,y)$ becomes

$$A\phi_{\xi\xi} + B\phi_{\xi\eta} + C\phi_{\eta\eta} + D\phi_{\xi} + E\phi_{\eta} = 0, \quad (2.11)$$

where $A = \xi_x^2 + \xi_y^2 = (x_\eta^2 + y_\eta^2)/J^2$, (2.12)

$$B = 2(\xi_x\eta_x + \xi_y\eta_y) = -2(x_\xi x_\eta + y_\xi y_\eta)/J^2, \quad (2.13)$$

$$C = \eta_x^2 + \eta_y^2 = (x_\xi^2 + y_\xi^2)/J^2, \quad (2.14)$$

$$D = \xi_{xx} + \xi_{yy}, \quad \left. \begin{array}{l} \\ \end{array} \right\} \text{(See Chu [5] for expression} \quad (2.15)$$

$$E = \eta_{xx} + \eta_{yy}. \quad \left. \begin{array}{l} \\ \end{array} \right\} \text{in terms of } x_\xi, y_\xi, \text{etc.)} \quad (2.16)$$

Similar expressions for more general equations than Laplace's can be developed, see Chu [5], Oberkampf [16], and these authors have shown that the equations do not change type (elliptic, hyperbolic or parabolic).

Corresponding transformations for normal derivatives of ϕ on the boundary follow from

$$\phi_n = \frac{1}{[(g')^2 + 1]^{\frac{1}{2}}} (g'\phi_x - \phi_y) \text{ on } y = g(x), \quad (2.17)$$

$$= \frac{1}{J[(g')^2 + 1]^{\frac{1}{2}}} \left[\phi_\xi(g'y_\eta + x_\eta) - \phi_\eta(g'y_\xi + x_\xi) \right] \quad (2.18)$$

where $g' = dy/dx$.

Time derivatives for the function $\phi(x,y,t)$ can be transformed from a given (x,y) point to the corresponding (ξ,η) point by the relation

$$\begin{aligned} (\phi_t)_{x,y} = (\phi_t)_{\xi,\eta} - \frac{1}{J} (y_\eta\phi_\xi - y_\xi\phi_\eta)(x_t)_{\xi,\eta} \\ - \frac{1}{J} (x_\xi\phi_\eta - x_\eta\phi_\xi)(y_t)_{\xi,\eta} \end{aligned} \quad (2.19)$$

and thus all derivatives of $\phi(x,y,t)$ can be expressed in terms of derivatives at fixed points in the transformed region even if the original mesh is moving (time-dependent).

The transformation functions $\xi(x,y)$ and $\eta(x,y)$ can be determined in various ways. Winslow [20], with later work by Chu [5], chose the mesh lines to be equipotential' lines where ξ and η satisfy

$$\nabla_{x,y}^2 \xi = 0, \quad \nabla_{x,y}^2 \eta = 0, \quad (2.20)$$

which makes x and y solutions of the quasilinear equations

$$\left. \begin{aligned} Ax\xi\xi + Bx\xi\eta + Cx\eta\eta &= 0, \\ Ay\xi\xi + By\xi\eta + Cy\eta\eta &= 0, \end{aligned} \right\} \quad (2.21)$$

and the governing equation for ϕ becomes

$$A\phi\xi\xi + B\phi\xi\eta + C\phi\eta\eta = 0. \quad (2.22)$$

The main advantage of using (2.20) is that (2.11) simplifies to (2.22) since $D = E = 0$. Also, Winslow notes that because of the averaging properties of solutions to Laplace's equation, it can be expected that a mesh constructed in this way is, in some sense, smooth. Winslow solved the quasilinear equations (2.21) by successive over-relaxation solution at each step of a corresponding sequence of linearised equations. Godunov and Prokopov [11] have used this method to construct moving meshes for time-dependent problems. Thompson et al. [19] have extended the above ideas to multi-connected regions and have shown how the spacing of the co-ordinate lines can easily be controlled by altering the elliptic system used to generate ξ and η .

Barfield [2] used an equivalent approach where x and y satisfied a linear elliptic system in the (ξ, η) plane, which

made (ξ, η) solutions of a quasi-linear system in the (x, y) plane, to produce a 'near orthogonal' (in the least squares sense), curvilinear mesh. Amsden and Hirt [1] used this approach to give a intuitively simple scheme for deforming a given regular (ξ, η) mesh into the required (x, y) mesh by moving the mesh points small steps at a time. Potter and Tuttle [17] have given an orthogonalisation procedure for the transformation of discrete nonorthogonal co-ordinates.

Instead of choosing ξ and η to satisfy (2.20), Oberkampf [16], used equations (2.11) - (2.16) with the mappings onto the unit square:

$$\xi = \frac{x - x_\ell(y)}{x_u(y) - x_\ell(y)} \quad , \quad (2.23)$$

$$\eta = \frac{y - y_\ell(x)}{y_u(x) - y_\ell(x)} \quad , \quad (2.24)$$

where x_ℓ, x_u, y_ℓ, y_u are the four curved sides in Figure 1.

In general, x_ℓ , etc. represent sets of discrete values of boundary points and are specifically chosen so as to give a required mesh spacing. Since ξ, η are then known (discrete) functions of x and y , the derivatives ξ_x, ξ_y , etc. required for the coefficient A-E are readily available by suitable discrete approximations. Alternative mappings than (2.23) and (2.24) are available by use of the finite element techniques of bivariate blending-functions, Gordon and Hall C-12J, or isoparametric curvilinear co-ordinates, Zienkiewicz and Phillips [21].

The choice of the use of orthogonal or nonorthogonal co-ordinates depends on the degree of sophistication required of the mesh generation

scheme. An orthogonal system cannot be achieved with arbitrary spacing of the natural co-ordinate lines around the boundary and, in certain situations, this capability is more important than orthogonality. However, nonorthogonal systems do involve more complicated governing equations and boundary conditions and greater overheads in the computation of the required transformation functions.

3. Model problem

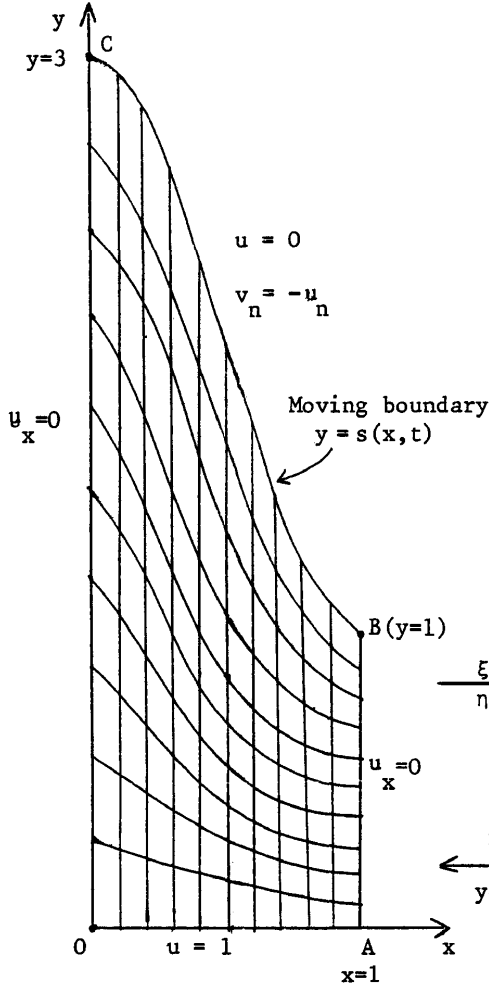


Figure 2. Physical plane.

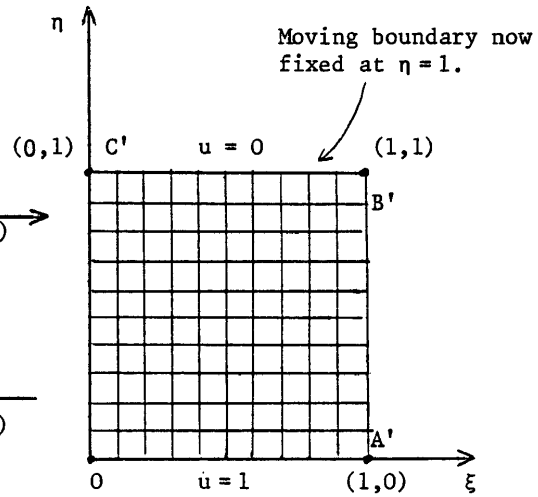


Figure 3. Transformed plane.

The one-phase, two-dimensional MBP of Bonnerot and Jamet [4] is taken as the model problem, see Figure 2. The problem is to solve for $u(x,y,t)$ and the MB $y = s(x,t)$

$$u_t = u_{xx} + u_{yy} \quad \text{in } 0 \leq x \leq 1, \quad 0 \leq y \leq s(x,t), \quad t > 0, \quad (3.1)$$

subject to

$$u_x = 0 \quad \text{on } x = 0 \quad \text{and } x = 1, \quad 0 \leq y \leq s(x,t), \quad t > 0, \quad (3.2)$$

$$u = 1 \quad \text{on } y = 0, \quad 0 \leq x \leq 1, \quad t > 0, \quad (3.3)$$

$$s(x,0) = 2 + \cos \pi x, \quad \left. \begin{array}{l} \text{initial conditions} \\ u(x,0) = 1 - y / (2 + \cos \pi x) \end{array} \right\} \quad 0 \leq x \leq 1, \quad 0 \leq y \leq s(x,0), \quad (3.4)$$

$$u(x,0) = 1 - y / (2 + \cos \pi x), \quad \left. \begin{array}{l} \text{initial conditions} \\ u(x,0) = 1 - y / (2 + \cos \pi x) \end{array} \right\} \quad 0 \leq x \leq 1, \quad 0 \leq y \leq s(x,0), \quad (3.5)$$

$$\left. \begin{array}{l} u = 0, \\ v_n = -u_n \end{array} \right\} \quad \text{on the MB } y = s(x, t), \quad t > 0, \quad (3.6)$$

$$(3.7)$$

where v_n denotes the velocity of the MB in the normal direction, n . The MB moves upwards and becomes the line $y = 4$ for $t > 7$.

The physical plane containing the curved MB is transformed into the unit square of Figure 3 using the transformations

$$\xi = x, \quad \eta = \eta(x, y) \quad (3.8)$$

Under these, in general, nonorthogonal transformations, the diffusion equation (3.1) becomes, from (2.11) and (2.19),

$$u_t = Au_{\xi\xi} + Bu_{\xi\eta} + Cu_{\eta\eta} + D'u_{\xi} + E'u_{\eta}, \quad 0 \leq \xi \leq 1, 0 \leq \eta \leq 1, t > 0, \quad (3.9)$$

$$\text{where } D' = D + \frac{1}{j}(x_{\eta}y_t - y_{\eta}x_t), \quad (3.10)$$

$$E' = E + \frac{1}{j}(y_{\xi}x_t - x_{\xi}y_t), \quad (3.11)$$

and A to E are given by (2.12) -(2.16).

Since $\xi = x$ these equations simplify to give

$$u_t = au_{\xi\xi} + bu_{\xi\eta} + cu_{\eta\eta} + du_{\xi} + eu_{\eta}, \quad 0 \leq \xi \leq 1, 0 \leq \eta \leq 1, t > 0, \quad (3.12)$$

$$\text{With } \left. \begin{array}{l} a = 1, b = -2y_{\xi}/y_{\eta}, \\ c = (1/y_{\eta})^2 + (b/2)^2, \quad d = 0, \\ e = n_{xx} + \eta_{yy} + y_t/y_{\eta}. \end{array} \right\} \quad (3.13)$$

and the boundary conditions (3.2) and (3.3) become

$$y_{\eta}u_{\xi} - y_{\xi}u_{\eta} = 0 \quad \text{on } \xi = 0 \text{ and } \xi = 1, \quad 0 \leq \eta \leq 1, t > 0, \quad (3.14)$$

$$u = 1 \quad \text{on } \eta = 0, \quad 0 \leq \xi \leq 1, \quad t > 0. \quad (3.15)$$

The MB condition (3.7) can be written in terms of movements along the y ordinates only, see [7,10], as

$$Y_t = -\{1 + (Y_x)^2\}u_Y, \quad \text{on } y = s(x, t). \quad (3.16)$$

From this the transformed MB conditions can be written as

$$\left. \begin{aligned} u &= 0 \\ y_t &= -\left(1 + y \frac{2}{\xi}\right) u_{\eta} / y_{\eta} \end{aligned} \right\} \text{ on } \eta = 1, t > 0. \quad (3.17)$$

$$(3.18)$$

The movement of the MB is now monitored by the change of y values for points (ξ, η) on $n = 1$ using (3.18).

4. Method 1 - solution based on transformations of Oberkampf [16],

Following the transformations of Oberkampf [16], equations (2.23) and (2.24) define the transformations

$$\xi = x, \quad \eta = y/s(x, t), \quad (4.1)$$

which is simply the two-dimensional version of the fixing of the boundary, Landau [15], transformation. (It has since been found that this idea has already been used by Duda et al. [8] for two-phase, two-dimensional MBPs.)

Using (4.1), the coefficients of the transformed diffusion equation (3.1) are, from (3.13) with $y_{\eta} = s$ and $y_{\xi} = ys_{\xi}/s$,

$$\left. \begin{aligned} a &= 1, \quad b = -2ys_{\xi}/s^2, \\ c &= (1/s^2) + (b/2)^2, \quad d = 0, \\ e &= (y/s)_{\xi\xi} + y_t/s, \end{aligned} \right\} \quad (4.2)$$

Similarly, the derivative boundary conditions (3.14) are

$$s u_{\xi} - (ys_{\xi} u_{\eta} / s) = 0 \text{ on } \xi = 0 \text{ and } \xi = 1 \quad (4.3)$$

and the MB condition (3.18) is

$$y_t = -\frac{1}{s} \left(1 + s \frac{2}{\xi}\right) u_{\eta}, \text{ on } \eta = 1. \quad (4.4)$$

If Figure 3 is discretised into a $N_1 \times N_2$ mesh of size h with $\xi_k = kh$, $k = 0, 1, \dots, N_1$, and $\eta_{\ell} = \ell h$, $\ell = 0, 1, \dots, N_2$, then

suitable discrete approximation for s_ξ , and $s_{\xi\xi}$ are

$$\left. \begin{aligned} s_\xi &= \frac{s_{k+1} - s_{k-1}}{2h}, \\ s_{\xi\xi} &= \frac{s_{k+1} - 2s_k + s_{k-1}}{h^2} \end{aligned} \right\} k = 1, 2, \dots, N_1 - 1. \quad (4.5)$$

At $k=0$ and $k=N_1$, $s_\xi = 0$ since $u_x = 0$ and $u = 0$.

The numerical solution proceeds by discretising the time variable t by $t^n = n\delta t$, $n = 0, 1, 2, \dots$ and by using suitable approximations for the derivatives of u over the unit square. Central finite-difference approximations, with simple explicit time-differencing approximations, are used in order to illustrate the ideas, the presence of the cross derivative term resulting in a nine-point formula. To maintain $O(h^2)$ accuracy for derivatives of u at the boundaries of the square, three-point end-on formulae may be used. Alternatively, use of the fictitious point idea results in two-point formulae which have the added advantage of possessing lower truncation error.

To develop fictitious point approximations for MB conditions of the form (4.4), i.e.

$$y_t = -k(\xi, t)u_\eta \text{ on } \eta = 1, t > 0, \quad (4.6)$$

it is necessary to combine (4.6) with the governing equation (3.12) applied at $\eta = 1$. This idea is well-known in heat conduction problems, Eyres et al. [9]. Combining (3.12) and (4.6) on $\eta = 1$ gives the tridiagonal system for the velocity y_t at the point ξ_k , notated by $(y_t)_k$,

$$-b(y_t/k)_{k-1} + (4c + 2eh)(y_t/k)_k + b(y_t/k)_{k+1} = -4c(u_{k,N_2} - u_{k,N_2-1})/h. \quad (4.7)$$

The tridiagonal system, rather than an explicit formula, arises because of the cross-derivative terms. This system is readily solved

using standard tridiagonal algorithms, and the position of the MB is given by the approximation

$$y_K^{n+1} = y_K^n + \delta t (y_t)_K, \text{ with error } O(\delta t + h^2). \quad (4.8)$$

The numerical solution algorithm is as follows:

- i) given u and s at time level n , relate (ξ, η) points to (x, y) points using (4.1) ;
- ii) compute the new position of the MB at time $(n+1)$ by a simple explicit approximation developed (a) from three-point end-on formulae for u or (b) from the fictitious point formulae (4,7) and (4.8) ;
- iii) use (4.1) to relate the changes in y at the points (ξ, η) ;
- iv) solve the diffusion equation (3.1) with coefficients (4.2) using a simple explicit time-differencing and (a) three-point or (b) fictitious point approximations at the boundaries. Go to step (ii) and repeat for each time level.

The results of the three-point, Method 1(a), and fictitious point, Method 1(b), schemes are compared in Table 1.

5. Method 2 - solution by 'equipotential' transformations, Winslow [20]

The 'equipotential' transformations (2.20) of Winslow [20] allow greater flexibility in the control of the mesh spacing, see the discussion in Thompson et al. [19]. Since $\xi = x$, the quasilinear system (2.21) for generation of the transformation reduces to the single quasilinear equation

$$\alpha y_{\xi\xi} - 2\beta y_{\xi\eta} + \gamma y_{\eta\eta} = 0, \quad (5.1)$$

$$\text{where } \alpha = y_{\eta}^2, \beta = y_{\xi} y_{\eta}, \gamma = 1 + y_{\xi}^2. \quad (5.2)$$

Control over the spacing of the co-ordinate lines is obtained by the choice of boundary points for the boundary conditions

$$\left. \begin{aligned} y = 0 \text{ on } \eta = 0, \quad y = \eta s(1, t) \text{ on } \xi = 1, \\ y = s(\xi, t) \text{ on } \eta = 1, \quad y = \eta s(0, t) \text{ on } \xi = 0, \end{aligned} \right\} \quad (5.3)$$

and by the addition of terms to the elliptic system (5.1), see Thompson et al.

The overheads of having to solve (5.1) at each time step are very expensive, and so an efficient numerical solution of (5.1) is a necessity. Winslow [201 and Chu [5] linearised the quasilinear equation (4.1) to the sequence of linear equations

$$\alpha^{(r-1)} y_{\xi\xi}^{(r)} - 2\beta^{(r-1)} y_{\xi\eta}^{(r)} + \gamma^{(r-1)} y_{\eta\eta}^{(r)} = 0, \quad r=1, 2, \dots, \quad (5.4)$$

and used successive over-relaxation, iterative solution for each linear equation. The coefficients α , β , γ at the next step r were under-relaxed using the scheme

$$\alpha^{(r)} = \rho \alpha(y^{(r)}) + (1-\rho)\alpha^{(r-1)}, \quad 0 < \rho < 1. \quad (5.5)$$

An advantage of co-ordinate transformation methods is that, for a reasonably accurate solution, the number of mesh points ($N_1 \times N_2$) in the transformed plane need not be very large, c.f. the large number of mesh points often needed in the physical plane. This suggests the use of a direct, rather than an iterative, solution of equations (5.4). With this in mind, a high-speed, banded matrix routine has been used for the solution of the nine-point, non-symmetric finite-difference equations resulting from central, finite-difference approximations of (5.1).

The numerical algorithm is then as for method (1) but with steps (i) and (iii) requiring the solution of (5.4) to determine the (ξ, η) transformation. Note that the set of co-ordinate lines generated by Methods 1 and 2 are different. This must be so since the transformations (4.1) of method 1 do not satisfy (2.20).

6. Numerical results and conclusions

Methods 1(a), 1(b) and 2(a) were programmed in Fortran on a CDC 7600 computer and the results are presented in Tables I and II. For methods of type (a), three-point end-on approximations are used for the derivatives at the boundaries. If the value of u_η is almost zero (as it is near $\xi = 0$ on $\eta = 1$ where the boundary is moving very slowly) then it was found that three-point approximations could give the wrong sign for u_η . If this happened then the 0(h) two-point end-on approximation was used since this always gave the correct sign. Methods of type (b) use the fictitious point approach described in section 4 and these methods always gave the correct sign for u_η . Explicit time-differencing schemes were used, the stability requirement being $\delta t \leq h^2/4$. Using this as an upper bound, the time step was successively halved until the values agreed to 4 significant figures.

The results are compared with those given by Bonnerot and Jamet [4] who used a finite-element method in both space and time based on an integral formulation of the problem. Their finite-element method uses a variable space, triangular mesh so that the MB is always approximated by a polygonal curve whose vertices are nodes of the triangulation. The use of finite elements in time results in a generalisation of the Crank-Nicolson implicit scheme. An explicit scheme is used to approximate the MB condition (3.7) and the MB position $y = s(x_k, t^n)$ is calculated from a geometrical procedure based

on approximations of u over the two adjoining straight line segments. Their best results ($\delta t = h = 1/64$) show good agreement with those of methods 1 and 2, but for smaller values of h and δt the agreement is not so good. Although the implicit method allows large time steps to be used, it is suggested that a smaller time step might give improved results for (say) $h = 1/16$.

Crowley (private communication) has applied both the enthalpy and the Isotherm Migration (IMM) methods described in Crank and Crowley [6] to this problem, and the results are compared in Tables I and II. The enthalpy formulation corresponding to the model problem was discretised using explicit finite-difference approximations and the position of the MB was located by extrapolation from the last two ($u > 0$) mesh points along each x line. The solution is over the fixed domain $\{0 \leq x \leq 1, 0 \leq y \leq 4\}$ thus necessitating 400 squares of side $h = 0.1$ for comparable accuracy to Methods 1 and 2. The IMM method uses the novel approach of working along the flow lines, orthogonal to the isotherms. This results in a locally one-dimensional, radial form of the IMM equation for the radius of curvature, r as a function of u and t . The values presented in Tables I and II are the results of early experiments and the authors expect that later experiments will improve the accuracy near $x = 0$. A further useful comparison would be the IMM method of Crank and Gupta [7], where y is expressed as a function of u , x and t .

Conclusions

Co-ordinate transformations based on Methods 1(a) and (b) provide a simple, efficient and accurate solution of the problem, with 1(b) being the most accurate. Method 2 is more expensive due

to the need to solve (5.1) at each time step but does offer a smoother and more flexible control over the curvilinear mesh spacing. Both methods compare favourably with those of Bonnerot and Jamet, Crank and Crowley, and can be readily extended to implicit schemes, e.g. see Duda et al. [8].

ACKNOWLEDGEMENT

I am grateful to Professor J. Crank for many valuable discussions and to Dr. A. B. Crowley for supplying the results of the enthalpy and IMM methods.

TABLE I - Comparison of Methods land 2 with those of Bonnerot and Jamet [4], Crank and Crowley [6]

Positions of the moving boundary $y = s(x, t)$ for $x = 0, 0.5$ and 1 at time $t = 2$.

Method	$s(0,t)$	$s(0.5,t)$	$s(1,t)$	Execution time per time step
Method 1(a), 100 squares of side $h=0.1$, $\delta t = 0.001$.	3.072	2.830	2.651	0.0017
Method 1(b), 100 squares of side $h=0.1$, $\delta t = 0.001$.	3.068	2.789	2.596	0.0017
Method 2(a), 100 squares of side $h=0.1$, $\delta t = 0.001$.	3.084	2.841	2.599	0.1325
Crank and Crowley enthalpy, 400 squares of side $h = 0.1$, $\delta t = 0.002$.	3.085	2.777	2.602	0.0147
Crank and Crowley IMM, 8 points on 5 isotherms ($\delta u=0.2$), $\delta t=0.0004$	3.248	-	2.523	0.0527
Bonnerot and Jamet, 256 triangles, $h = \delta t = 1/16$,	3.122	2.902	2.679	0.0367
4096 triangles, $h = \delta t = 1/64$.	3.068	2.810	2.610	-

Notes

The execution times are all for runs on a CDC 7600 computer. The only execution time quoted by Bonnerot and Jamet is for 200 triangles with $h = \delta t = 1/10$, so this value has been scaled up to 256 triangles. Method 2(a) involves on average 6 iterations of (5.4) to obtain convergence of the y values to an accuracy of 10^{-6} .

TABLE II - Comparison of successive mesh refinements

Positions of the moving boundary $y=s(x,t)$ for $x = 0, 0.5$ and 1 at time $t = 2$.

Method	$s(0,t)$	$s(0.5,t)$	$s(1,t)$
Method 1(a) $\left\{ \begin{array}{l} h = 1/8 \\ h = 1/16 \\ h = 1/32 \end{array} \right.$	3.089 3.053 3.052	2.866 2.797 2.780	2.685 2.610 2.587
Method 1(b) $\left\{ \begin{array}{l} h = 1/8 \\ h = 1/16 \\ h = 1/32 \end{array} \right.$	3.068 3.066 3.062	2.794 2.781 2.777	2.600 2.589 2.585
Crank and Crowley [6], enthalpy method $\left\{ \begin{array}{l} h = 1/10 \\ h = 1/16 \end{array} \right.$	3.085 3.051	2.777 2.799	2.602 2.566
Bonnerot and Jamet [4], finite-element method $\left\{ \begin{array}{l} h = 1/8 \\ h = 1/16 \\ h = 1/32 \\ h = 1/64 \end{array} \right.$	3.181 3.122 3.085 3.068	2.978 2.902 2.843 2.810	2.712 2.679 2.635 2.610

REFERENCES

1. A. A. Amsden and C. W. Hirt, J. Comp. Phys. 11 (1973), 348-359.
2. W. D. Barfield, J. Comp. Phys. 6 (1970), 417-429;
also *ibid* 5 (1970), 23-33.
3. J. D. Boadway, Int. J. Num. Meth. Engng. 10 (1976), 527-533.
4. R. Bonnerot and P. Jamet, J. Comp. Phys. (to appear).
5. W - H Chu, J. Comp. Phys. 8 (1971), 392-408.
6. J. Crank and A. B. Crowley, Brunei University Math. Report TR/70;
also Int. J. Heat Mass Transfer (to appear).
7. J. Crank and R. S. Gupta, Int. J. Heat Mass Transfer 18 (1975),
1101 - 1107.
8. J. L. Duda, M. F. Malone, R. H. Notter and J. S. Ventras,
Int. J. Heat Mass Transfer 18 (1975), 901 - 910.
9. N. R. Eyres, D. R. Hartree, J. Ingham, R. Jackson, R. J. Sarjant
and J. B. Wagstaff, Phil. Trans. Roy. Soc. 240A (1946), 1-57.
10. R. M. Furzeland, Brunei University, Math. Report TR/76 (1977).
11. S. K. Godunov and G. P. Prokopov, USSR Comp. Math. Math. Phys. 12
(1972), 182-195.
12. W. J. Gordon and C. A. Hall, Int. J. Num. Meth. Engng. 7 (1973),
461-477.
13. T-K. Hung and T. D. Brown, J. Comp. Phys. 23 (1977), 343-363.
14. P. G. Kroeger and S. Ostrach, Int. J. Heat Mass Transfer 17
(1974), 1191-1207.
15. H. G. Landau, Q. Appl. Math. 8 (1950), 81-94.
16. W. I. Oberkampf, Int. J. Num. Meth. Engng. 10 (1976), 211-223.
17. D. E. Potter and G. H. Tuttle, J. Comp. Phys. 13 (1973), 483-501.
18. A. Thorn and C. J. Apelt, "Field Computations in Engineering and
Physics", van Nostrand, London, 1961.
19. J. F. Thompson, F. C. Thames and C. W. Mastin, J. Comp. Phys. 15,
(1974), 299-319.
20. A. M. Winslow, J. Comp. Phys. 2 (1967), 149-172.
21. O. C. Zienkiewicz and D. V. Phillips, Int. J. Num. Meth. Engng. 3
(1971), 519-528.

